ELSEVIER

Journal of Chromatography A, 769 (1997) 81–92

JOURNAL OF CHROMATOGRAPHY A

Dynamic simulation of simulated moving-bed chromatographic processes for the optimization of chiral separations

J. Strube[a,*], U. Altenhöner[a], M. Meurer[a], H. Schmidt-Traub[a], M. Schulte[b]

[a]*University of Dortmund, Department of Chemical Engineering, 44221 Dortmund, Germany*

[b]*Merck KGaA, LPRO CHROM, Research and Development, 64271 Darmstadt, Germany*

Abstract

Mass separation by simulated moving-bed (SMB) chromatographic processes is influenced by a number of different parameters. Therefore planning and realization of pilot experiments as well as process design and optimization are complicated tasks. Todays new applications of SMB processes in the pharmaceutical, agrochemical and biochemical production have to deal with concentration-dependent capacity and separation factors near unity and have to be operated at high resolution, yield and purity. Therefore rigorous dynamic process modelling combined with a few characteristic experiments to determine the model parameters which describe axial dispersion, multi-component equilibrium with interference of the components and mass transfer resistances has proved necessary. The detailed dynamic model which has been developed is a crucial aid in understanding malfunctions of pilot plants, optimizing process conditions and specifying start-up procedures for SMB processes. This paper presents a first study to verify the rigorous dynamic SMB process model by experimental data of a SMB process. The proposed modelling approach, method of model parameter estimation and process optimization are verified by experimental data of an enantioseparation. The model parameters are estimated by experiments at an analytical HPLC single column and a pilot pulse through the SMB columns. Experimental process data are used to compare the results of process simulations with measured axial concentration profiles.

Keywords: Simulated moving-bed chromatography; Preparative chromatography; Enantiomer separation; Adsorption isotherms; Computer simulation; Optimization

1. Introduction

The simulated moving-bed (SMB) process is a powerful tool for continuous separation of multi-component mixtures with components of different adsorption affinities. It is suitable for a broad range of preparative and production scale applications and allows the separation of components with separation factors near unity, providing high resolution, yield and purity. Furthermore, the desorbent rates and the amount of adsorbent required by SMB processes are much lower than those for corresponding batch processes [1]. Today, new preparative applications of SMB processes are under development for the separation of racemic mixtures at very high purity [2,3].

The SMB process depends on different parameters specifying (i) plant size, (ii) operating conditions and (ii) process variables.

*Corresponding author.

PII S0021-9673(97)00236-7

Rigorous simulations are necessary for process design and evaluation of experimental results.

2. Simulation results

2.1. Modelling approaches

Different models have been evaluated which describe the chromatographic process in terms of either *moving beds* with steady state counter-current flow or *simulated moving beds* with periodic fluid port switching.

In order to develop an useful and reliable model for the simulation of SMB plants, the most common models have been programmed and evaluated [4,5]. The simulation package SPEEDUP (AspenTec) has been used as a solver.

The moving bed (MB) process description (Fig. 1) constitutes the theoretical extreme of a SMB process (Fig. 2) with an infinite number of columns and infinitesimal column length and switching time.

If the operating conditions are chosen correctly, the more adsorbable components of the feed stream accumulate in the extract stream, whereas the less adsorbable ones accumulate in the raffinate stream. A desorbent is needed to regenerate the adsorbent and to improve the separation.

These four external fluid streams divide the chromatographic unit into four different sections:

In section I the more strongly adsorbed component A is desorbed, whereas in section II the more weakly adsorbed component B is desorbed. Feed enters between sections II and III. Component A is adsorbed in section III, while component B with a weaker adsorption affinity is adsorbed in section IV. Thus in sections II and III the feed components are separated, while section I is used to regenerate the adsorbent and section IV to regain the desorbent.

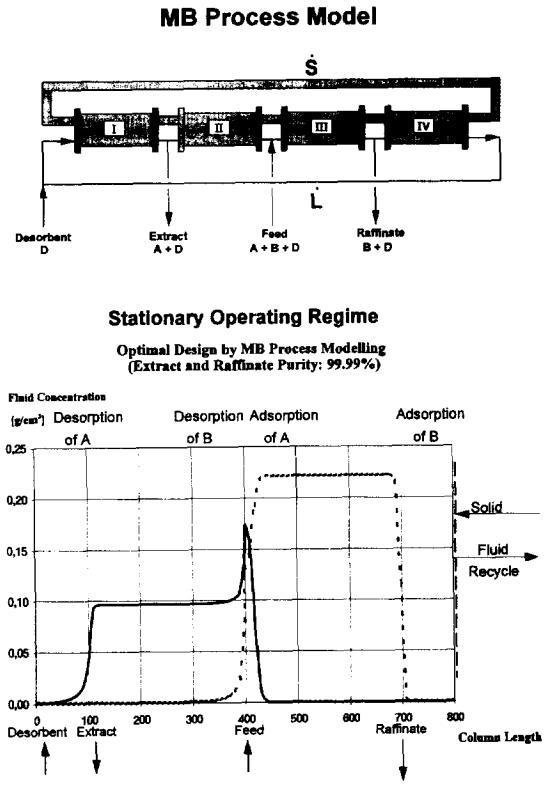

Fig. 1. MB process model — simulation. ——— Component A, - - - component B.

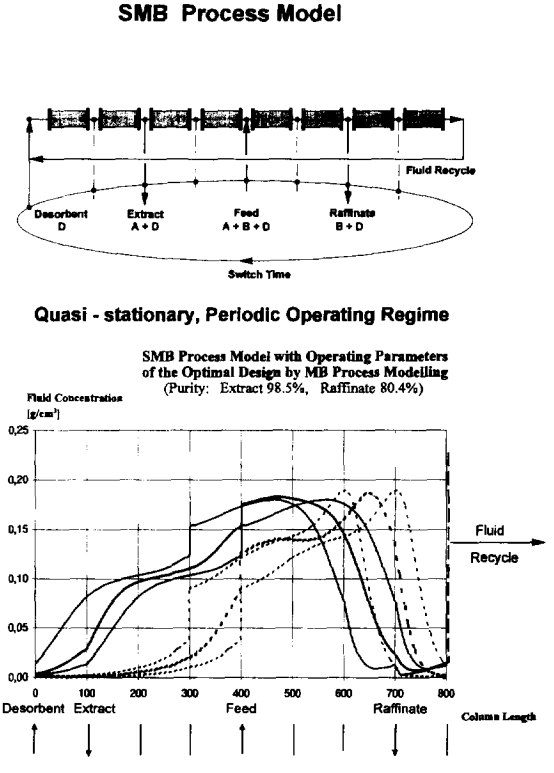

Fig. 2. SMB process model — simulation. ——— Component A, - - - component B (beginning, middle and end of a period in steady-state).

The MB process with steady state counter-current flow of fluid and solid is not practicable. It can, however, be approximated by the SMB process (Fig. 2) where packed solid beds are used and the locations of the inlet and outlet ports are switched periodically in the same direction as the fluid flow.

The SMB process was initially developed to separate isomeric mixtures such as xylenes or sugars using resins and zeolites. Several applications have been described in literature since "Sorbex" process types were developed by UOP [1]. Here, liquid-phase separation is carried out by a large number of columns in order to approximate true counter-current flow of solid and liquid as well as possible [6–8].

Today, new applications for pharmaceutical and biochemical products are under development for the separation of racemic mixtures at very high purity. Continuous chromatography is an efficient alternative for the separation of optically active enantiomers in comparison to selective crystallization or kinetic resolution [9].

Provided SMB processes are running in a quasi-steady state mode, the product concentrations change in a cyclic manner due to the periodic movement of the external input and outlet ports along the sequence of columns. In contrast to this cyclic behaviour, the stationary regime of the MB processes is independent of time.

The successful design and operation of counter-current separation units depend on the correct choice of operating conditions, in particular on the flow-rates in each section. Because of the complex behaviour of these units, the choice of the operating conditions is not straightforward.

In order to find out which models are useful and reliable for the simulation of SMB plants, the most common models have been programmed and compared to each other [5].

2.1.1. Rigorous dynamic SMB process model (Fig. 2)

DPF model

Fluid mass balance including mass transfer resistance:

$$\frac{\partial c_i}{\partial t} = D_L \frac{\partial^2 c_i}{\partial z^2} - \frac{\partial v c_i}{\partial z} - \frac{1-\epsilon}{\epsilon} \frac{3 k_{\mathrm{eff}_i}}{R_P} (c_i - c_{P_i}) \qquad (1)$$

Particle mass balance including mass transfer resistance:

$$\frac{\partial q_i}{\partial t} = k_{\mathrm{eff}_i} \frac{3}{R_P} (c_i - c_{P_i}) \qquad (2)$$

Isotherms:

$$q_i = f(c_{P_1}, \ldots, c_{P_{NC}}) \quad \text{with } i = 1, \ldots, NC \qquad (3)$$

2.1.2. Numerical methodology

The partial differential equations (PDEs) are transferred into ordinary differential equations (ODEs) by the method of lines or orthogonal collocation. Various types of finite difference formulas in axial space have been analysed to achieve a robust numerical solution of the sparse and stiff differential algebraic equation (DAE) systems. The Leonard difference scheme proved to be robust, exact and fast in time and space domains. Modified Danckwerts boundaries are used.

The simulation package SPEEDUP is used to solve the ODEs. The numerical methodology allows to calculate the periodic discontinuities caused by the discrete fluid port switching of SMB processes.

During the simulation studies it proved necessary to extend the simulation system in order to vary the total number of columns and the number of columns in each section. The flowsheets of the different processes are compiled automatically.

The simulation system, however, allows any isotherm to be used to consider the specific behaviour of the components.

2.2. Process optimization

Based on systematic parameter studies, a strategy has been developed to optimize the separation of SMB processes with the aid of a rigorous dynamic SMB process model [10]:

At first, flow-rates are estimated by the MB modelling approach assuming instantaneous equilibrium between the phases. These estimates are then refined using the rigorous dynamic SMB model for detailed optimization. Optimization targets are (i) maximum feed as well as (ii) minimal dilution of the products, (iii) minimal adsorbent requirement and (iv) minimal desorbent requirement.

The first approach was to optimize the SMB

process using the MB process model. For a given set of process parameters (eight columns, regular segmentation, column length and diameter) extract and raffinate purities of 99.99% are achieved at minimal desorbent requirement, product dilution and maximal feed throughput. The corresponding axial profile is shown in Fig. 1. Afterwards these operating parameters are used as input data for a SMB process model. The simulated axial profiles are presented in Fig. 2. Here extract purity decreases to 98.5% and raffinate purity to 80.4%. Furthermore, maximal feed throughput, minimal desorbent requirement and dilution are not reached. A new set of parameters has to be determined to achieve optimal production of the SMB plant. As a final result of the optimization procedure the feed throughput has to be decreased about 60% and the desorbent requirement increases to about 300% to achieve total separation of the products.

These results demonstrate that because of the periodic flow, SMB processes have to be described by rigorous dynamic models. These models have to take into account axial dispersion and mass transfer resistance in order to obtain good agreement with experimental results.

The rigorous modelling approach also delivers essential information for a better understanding of the chromatographic processes. Therefore, it is crucial to (i) plan experiments, (ii) understand malfunctions of pilot plants, (iii) optimize process conditions, (iv) develop control strategies and (v) analyse start-up procedure and stability of SMB processes.

Simulation studies prove that eight columns in regular segmentation are sufficient to achieve complete separation of the feed components and minimize dilution and desorbent requirement at maximal feed throughput. The required column length is a function of the separation factor and the column diameter is proportional to the throughput.

In order to optimize todays new applications of SMB processes, rigorous dynamic process modelling combined with a few characteristic experiments are necessary. These experiments are used to determine the model parameters which describe (i) axial dispersion, (ii) multi-component equilibrium with interference between the components and (iii) mass transfer resistances.

The methodology to determine the model parameters is described in detail in an additional paper [11]. The sensitivity and the magnitude of the model parameters are presented in [12]. But, for enantioseparations there are not yet published any comparisons of experimental and simulated SMB processes to verify the proposed methodology of model parameter estimation, necessary process modelling approach and optimization strategy.

3. Model verification for enantioseparations

3.1. Estimation of the model parameters

Due to the high costs of products only minimal amounts of feed should be used to determine the model parameters. Moreover, it is costly to separate single components of the racemic mixtures. As far as possible, the measurements should be carried out with racemic mixtures.

It is necessary to develop a methodology for the estimation of model parameters, taking into account these limitations of racemic mixtures.

This approach to estimate model parameters by minimal efforts has to be seen in contrast to the sophisticated approach to determine consistent model parameters presented in [11].

3.1.1. Example: enantioseparation of EMD 53986

EMD 53998 is the first compound of a new class of cardiotonic agents that shows a very interesting dual mechanism of action: the (+)-enantiomer of EMD 53998 is a potent Ca-sensitizing drug, whereas the (−)-enantiomer is a pure PDE III inhibitor devoid of any Ca-sensitizing activity [13].

The synthesis of both enantiomers of EMD 53998 is performed via separation of the enantiomers of the synthesis intermediate EMD 53986.

Here the separation on a stationary phase with a poly[N-acryloyl-amino acid-ester] chiral stationary phase as a chiral selector (Chiraspher type) is presented. As mobile phase, ethyl acetate with 5% ethanol is suitable. The preparative scale separation is performed on a Licosep 12-26 SMB. Eight columns are used ($L = 5.3$ cm). The experimental conditions and the experiments are described in detail in [13]. Consequently here they are only summarized.

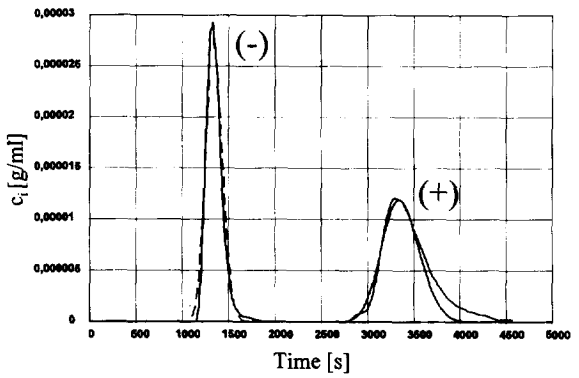

Fig. 3. Pilot pulse — experiment and simulation. ——— Experiment, - - - simulation (parameters of Table 1, volume flow 28.6 ml/min, injection time 1.05 s). [$K_{H(+)}=11.33$, $K_{H(-)}=4.12$, $k_{eff(+)}=3\cdot10^{-4}$ cm/s, $k_{eff(-)}=2.5\cdot10^{-4}$ cm/s].

3.1.2. Minimal set of experiments

First step: a pilot pulse through the eight SMB-columns is performed to determine the Henry-coefficients and mass transfer resistance coefficients. Axial dispersion coefficients are calculated by the Butt–Schneider correlation [14].

The Henry-coefficients and mass transfer resistance coefficients are determined by simulation of the pilot pulse (Fig. 3).

The retention times of both components fit well with the measured data. Only small deviations occur at the desorption front of the (+)-enantiomer. The linearized, overall mass transfer coefficients which are assumed could not describe the extreme tailing of this desorption front.

The sensitivity of the axial dispersion and the mass transfer coefficients are shown in Figs. 4 and 5. The magnitudes are physically realistic: mass transfer coefficients in the area of 10^{-4} cm/s are typical for kinetically dominated chromatographic separations. Instantaneous equilibrium is reached with coefficients greater than 10^{-2} cm/s whereas coefficients smaller than 10^{-6} cm/s correspond to no adsorption at all. These are the extreme cases and limitations.

An axial dispersion coefficient of $4.5\cdot10^{-4}$ cm^2/s

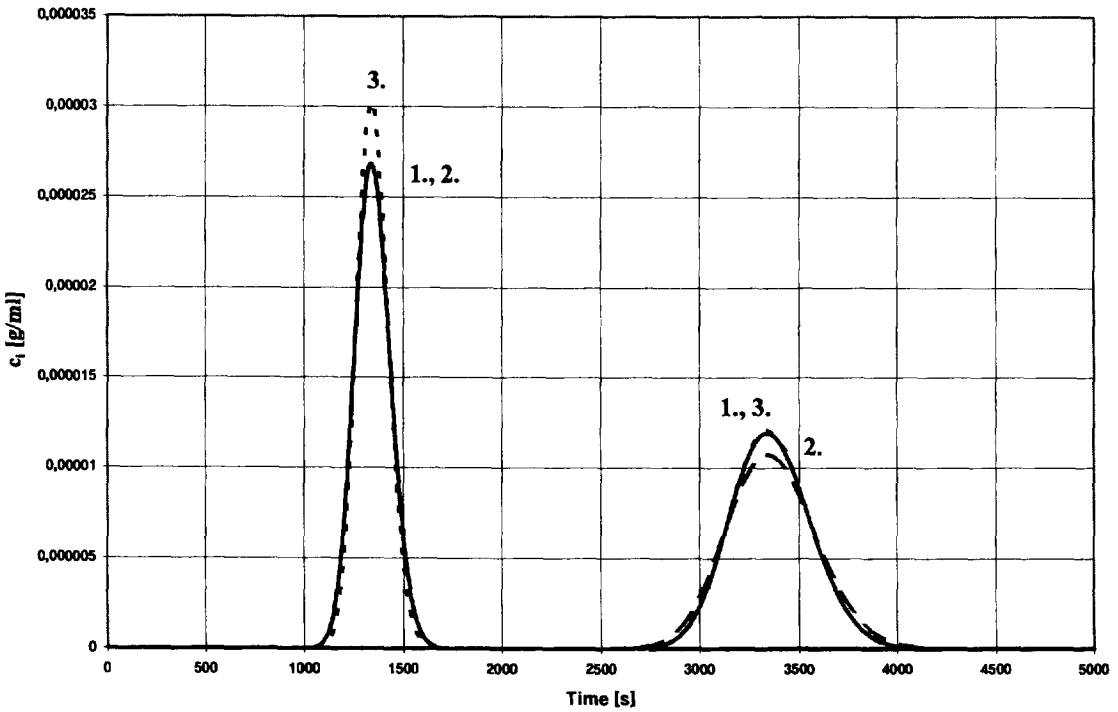

Fig. 4. Pilot pulse — sensitivity to axial dispersion. (1) Parameters of Table 1, (2) D_L changed to $4.5\cdot10^{-3}$ cm^2/s, (3) D_L changed to $4.5\cdot10^{-5}$ cm^2/s.

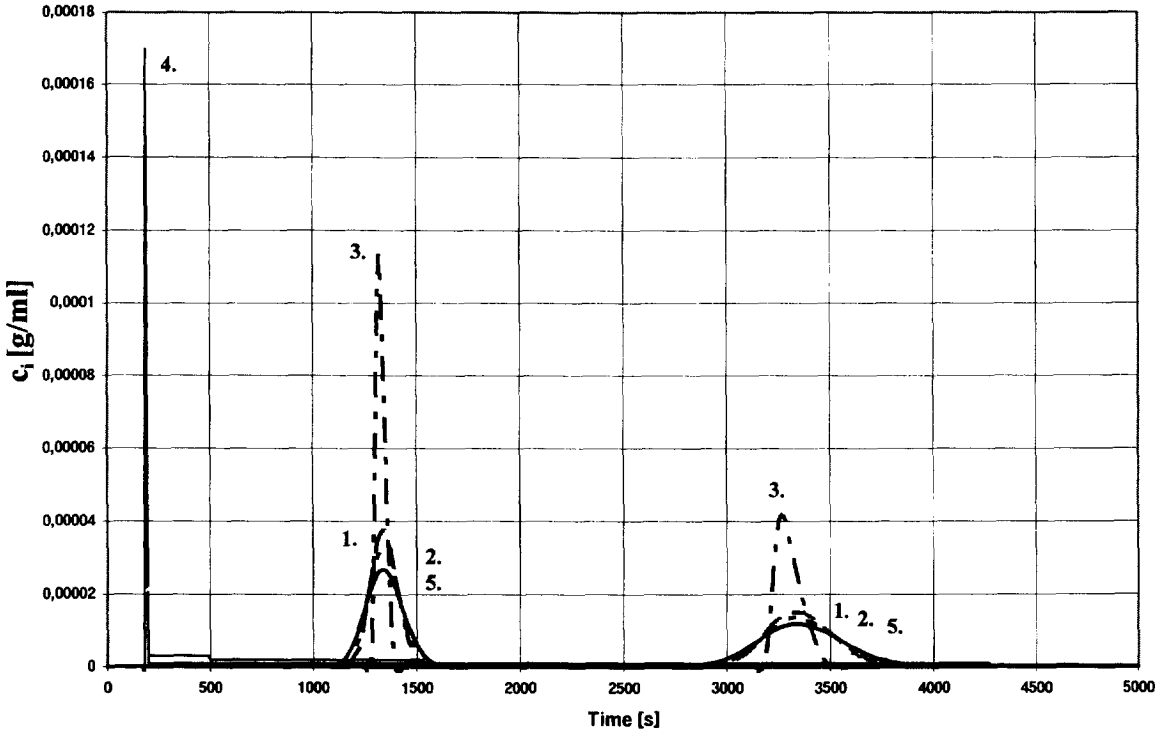

Fig. 5. Pilot pulse — sensitivity to mass transfer resistance. (1) Parameters of Table 1 and $k_{eff,i}$ changed to $5 \cdot 10^{-4}$ cm/s, (2) $k_{eff,i}$ changed to $4 \cdot 10^{-4}$ cm/s, (3) $k_{eff,i}$ changed to $1 \cdot 10^{-2}$ cm/s, (4) $k_{eff,i}$ changed to $1 \cdot 10^{-6}$ cm/s, (5) parameters of Table 1.

is calculated by the Butt–Schneider correlation. As this racemic system is kinetically controlled, the effects of the axial dispersion coefficient are not very sensitive. These results are in accordance with [12] where sensitivity and magnitude of these parameters are presented as well.

Second step: in an analytical HPLC column the following experiments are carried out to estimate the isotherms: two adsorption/desorption measurements of pure components at maximum concentrations and one adsorption/desorption measurement of racemic mixtures at maximum concentration.

3.1.3. Choice of the isotherm type and determination of the isotherm coefficients

Due to the results of Ching et al. [15] for enantioseparations it is sensible to assume modified Langmuir isotherms (Fig. 6):

$$q_i = P_i c_i + \frac{a_i c_i}{\left(1 + \sum_{j=1}^{NC} b_j c_j\right)} \quad \text{with } i = 1,\ldots, \text{NC} \qquad (4)$$

Different types like Henry, Langmuir and modified Langmuir isotherms have been tested. But, only modified Langmuir isotherms are capable of regressing the experiments and describing the SMB process behaviour as well. Because the separation factor

$$\alpha = \frac{dq_A}{dc_A} / \frac{dq_B}{dc_B} \qquad (5)$$

(with A more strongly adsorbable than B) depends on concentration and approximates to unity at higher concentrations (Fig. 6).

To determine the missing coefficients of the modified Langmuir isotherm, measurements of the

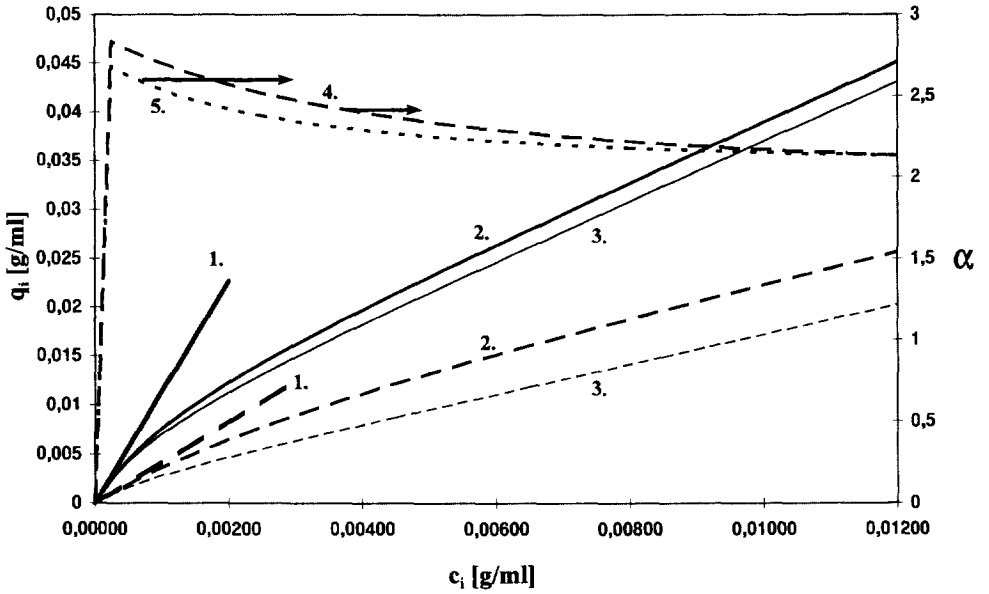

Fig. 6. Modified Langmuir isotherm and separation factor. ——— Component A(+), - - - component B(−). (1) Henry isotherm, (2) modified Langmuir isotherm for pure components, (3) modified Langmuir isotherm for identical component concentrations, (4) separation factor of the modified Langmuir isotherm for pure components, (5) separation factor of the modified Langmuir isotherm for identical component concentrations.

pure components at high concentration and of mixtures over the concentration range are necessary. A good regression of the concentration-dependent separation factor is essential for the simulation results (Fig. 7). This is documented in Fig. 8. The simulation results with a Henry, a Langmuir and a modified Langmuir isotherm which are fitted to the experiments [13] on the HPLC are presented. It is obvious that only the modified Langmuir isotherm type is capable to describe the correct mass separation of the SMB process. Selective and nonselective adsorption sides have to be considered to predict the separation factor which depends on the concentration (Fig. 6). The linear term of the modified Langmuir isotherm is absolutely necessary because the pure Langmuir isotherm predicts too steep adsorption fronts. Henry isotherms are not suitable because the extreme interference of the components could not be described. This equilibrium behaviour is quite usual for enantioseparations [3,15,9].

The complete set of model parameters is listed in Table 1. The solubility of the single component is about 12 g/l. The feed concentration is chosen as large as possible to increase feed throughput.

3.2. Verification of the SMB process model

Three different sets of operation parameters are simulated (Table 2). The simulation results fit the experimental concentration profiles quite well (Figs. 9–11). The axial concentration profiles are measured at half time of a period. To compare simulated and experimental results simulated concentration profiles of a stable steady-state are shown at the beginning, middle and end of a switch period.

4. Discussion

The concentration plateaus of extract and raffinate are not described very well. But the break through points of the four corresponding concentration waves

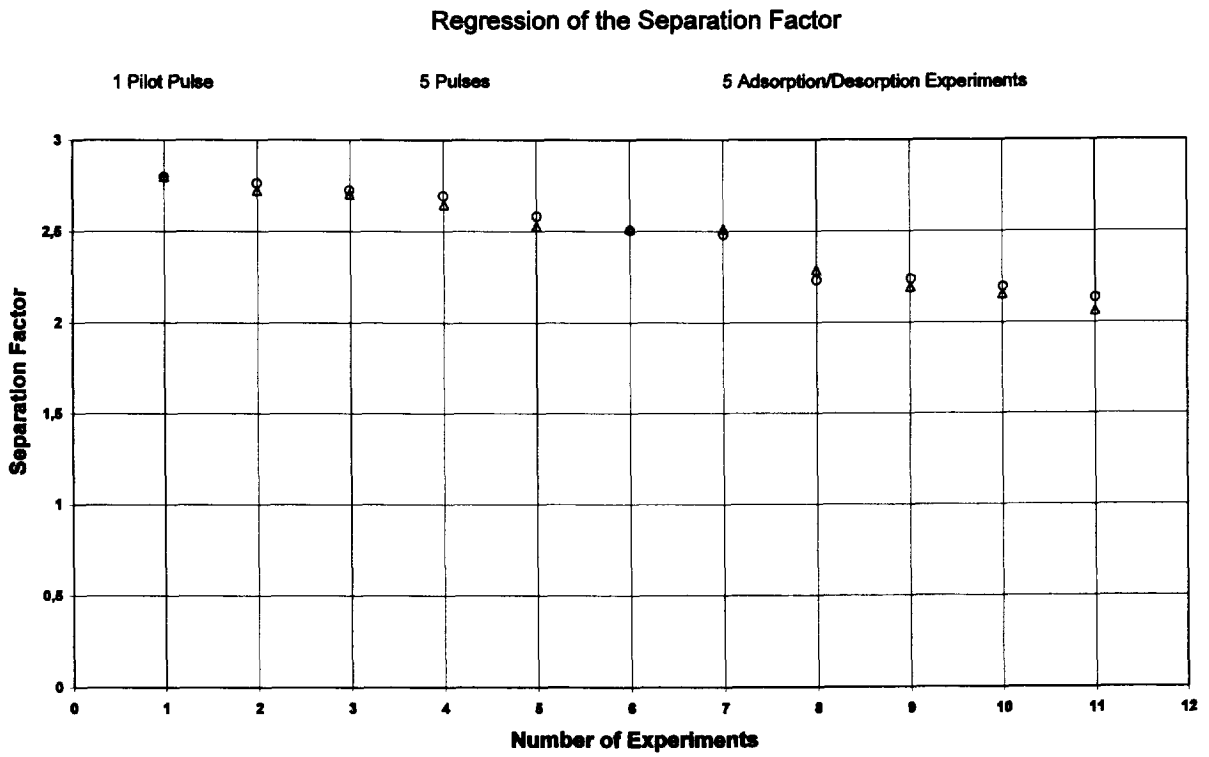

Fig. 7. Regression of the separation factor. △ Measured separation factor, ○ calculated separation factor. Concentration increases from Henry region (Experiment No. 1) to maximal solubility (Experiment No. 11).

in the SMB processes at low concentrations are simulated well with all three parameter sets. The extract and raffinate purities could be predicted.

It has to be taken into account:

(1) The single measurement of the axial profiles at half time of a period is not very exact because it has to be proved that a stable steady-state is reached. Little deviations in time lead to great errors in the axial profile.

(2) The model parameters are estimated quite rough. A more sophisticated approach to determine consistent model parameters is described in [11]. This will lead to a better agreement with experimental results. As the system is kinetically controlled the sensitivity to deviations of the axial dispersion coefficient is not very high. Errors in the simulated axial concentration profile could not occur due to these phenomena. In this case the rough experimental parameter estimation is quite sufficient, but the isotherms should be determined more exactly over the whole concentration range.

(3) Moreover, dead volumes of the SMB plant have to be taken into account to achieve a better correspondence with experimental results. In the simulation system these nonidealities are already programmed. But, for this example experimental data is yet lacking. Therefore, tracer tests will be done to determine the relevant dead volumes of the SMB plant and the nonconformity of the column packings. These nonidealities will be added in the process description.

(4) For process design and optimization by simulation studies it is helpful that an exact description of the break through points at low concentrations is

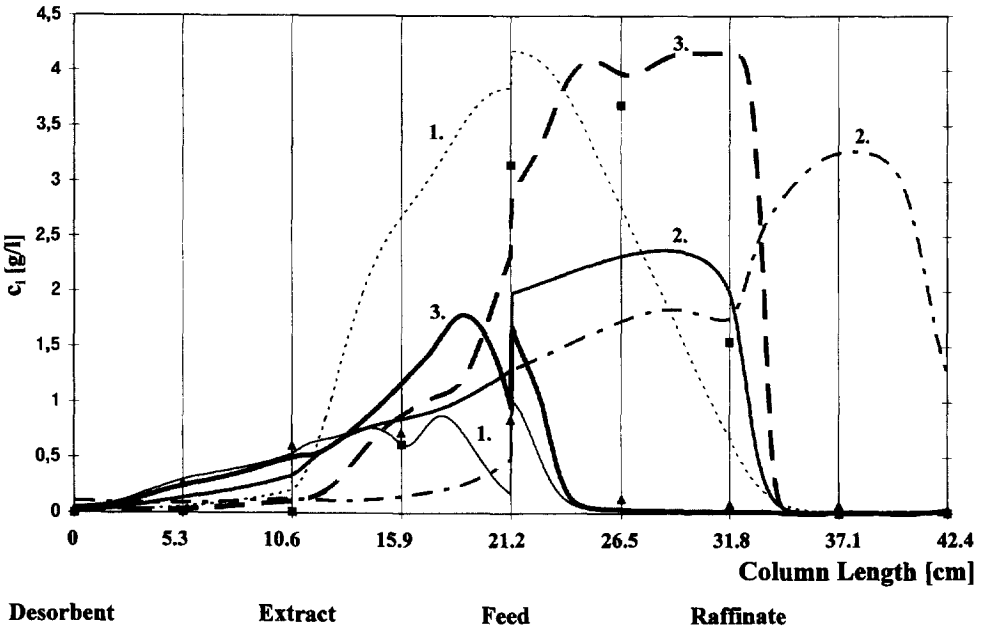

Fig. 8. Axial profile of the SMB process — operation parameter Set 3. ——— Component A(+), - - - component B(−). Comparison of experiment (▲ extract and ■ raffinate at the middle of a period) and simulations with (1) Henry, (2) Langmuir and (3) modified Langmuir isotherms—at the middle of a period in steady-state.

essential because deviations would lead to a wrong prediction of the product purities. An exact prediction of the concentration plateaus of extract and raffinate is of course desirable but at first not essential.

Table 1
Model parameters

Columns	8
Segmentation	2:2:2:2
D_{column}	2.6 (cm)
L_{column}	5.3 (cm)
D_L	$4.5 \cdot 10^{-4}$ (cm^2/s)
$k_{eff,A}$	$3 \cdot 10^{-4}$ (cm/s)
$k_{eff,B}$	$2.5 \cdot 10^{-4}$ (cm/s)
d_p	10 (μm)
ϵ	0.4
P_A	3
a_A	8.33
P_B	1.5
a_B	2.62
b_A	830 (cm^3/g)
b_B	260 (cm^3/g)

5. Conclusions

In addition to a sophisticated method to determine consistent model parameters of high accuracy [11] a short-cut methodology is proposed to estimate roughly model parameters by taking into account the limitations of racemic mixtures:

(1) A pilot pulse with the racemic mixture at maximum solubility is performed to estimate the Henry- and the mass transfer resistance-coefficients. The dispersion is calculated by the Butt–Schneider

Table 2
Operation parameters of the SMB processes

	Set 1	Set 2	Set 3
Desorbent (ml/min)	23.67	23.67	22.8
Extract (ml/min)	18.63	19.93	20.64
Feed (ml/min)	1.66	1.66	1.84
$c_{Feed,i}$ (g/l)	6.27	6.27	6.27
Raffinate (ml/min)	6.7	5.4	4.0
Switch time (min)	7.03	7.03	7.03

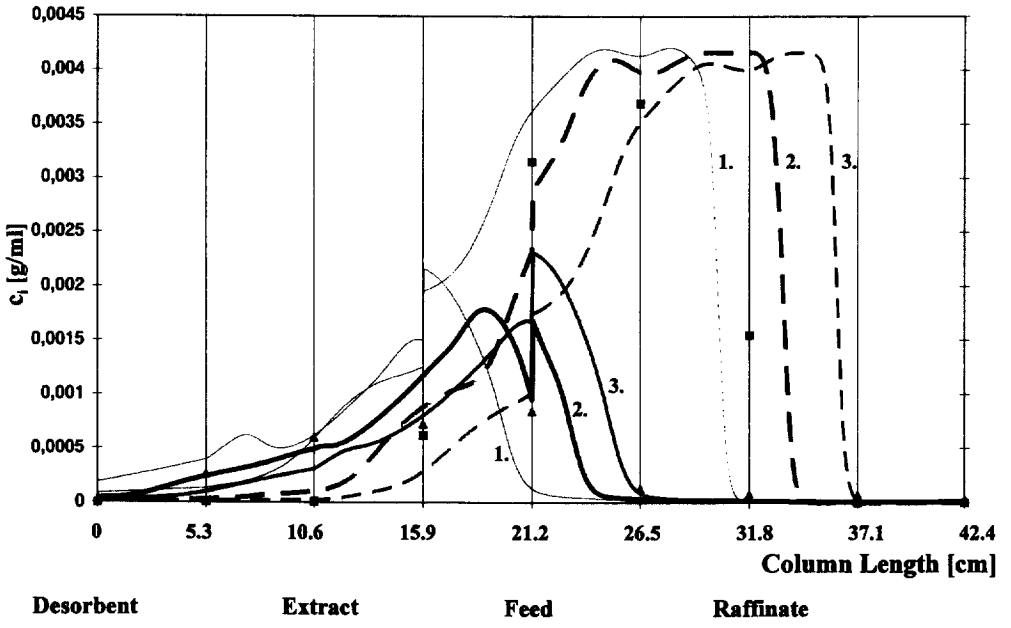

Fig. 9. Axial profile of the SMB process — operation parameter Set 3. ——— Component A(+), - - - component B(−). Comparison of experiment (▲ extract and ■ raffinate at the middle of a period) and simulation with modified Langmuir isotherms. (1) Beginning of a period, (2) middle of a period, (3) end of a period.

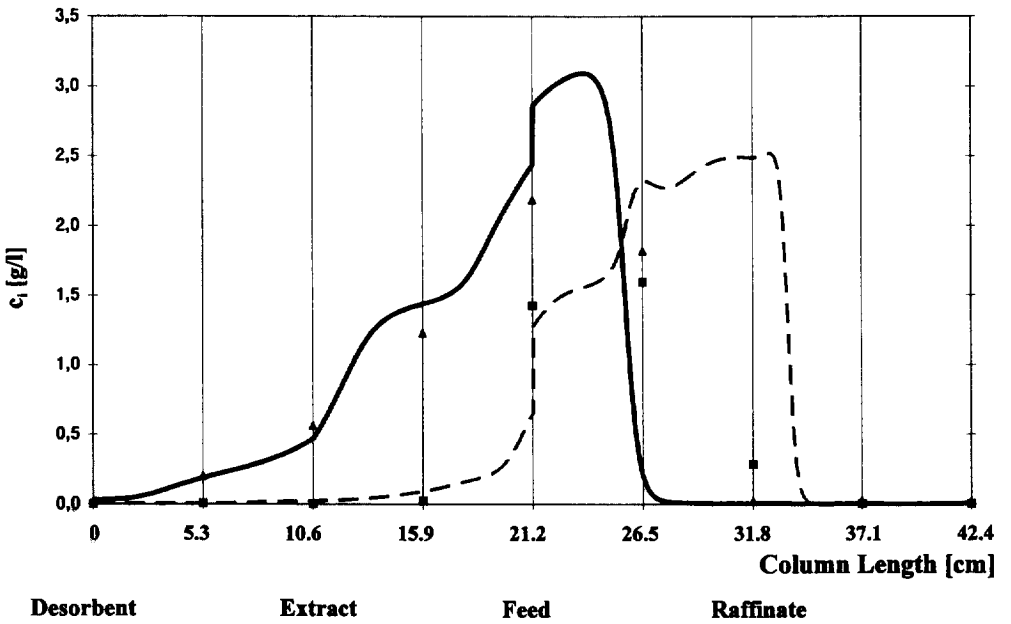

Fig. 10. Axial profile of the SMB process — operation parameter Set 1. ——— Component A(+), - - - component B(−). Comparison of experiment (▲ extract and ■ raffinate at the middle of a period) and simulation with modified Langmuir isotherms—at the middle of a period.

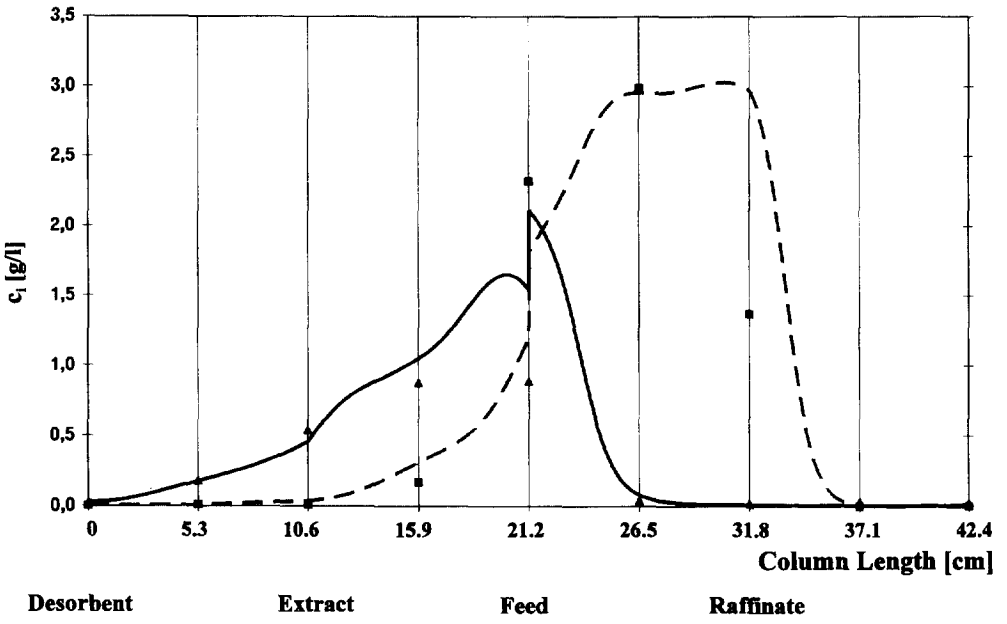

Fig. 11. Axial profile of the SMB process — operation parameter Set 2. ——— Component A(+), - - - component B(−). Comparison of experiment (▲ extract and ■ raffinate at the middle of a period) and simulation with modified Langmuir isotherms — at the middle of a period.

correlation and the linearised driving force approach is assumed.

(2) Modified Langmuir-isotherms are assumed to describe the selective and nonselective adsorption behaviour of enantiomers. The Langmuir-coefficients are determined by an experiment with the single components at an analytical column at maximum concentration.

(3) The interference coefficients of the modified Langmuir-isotherm are measured at the analytical column with maximum concentration of the racemic mixture.

The initial operating parameters are calculated by the method of Nicoud and coworkers [16,9]. Extract purity of 96.7% and raffinate purity of 96.6% are achieved in reality and simulation. Further optimization is necessary as product purity greater than 99.9% is demanded. If the separation system is kinetically controlled and if nonlinear isotherms are valid the sensitivity to axial dispersion is not extremely high, but even small dead volumes in the plant have to be modelled. The simulations will be concluded taking into account relevant dead volumes and nonconformity of the column packings of the simulated SMB plant.

The proposed short-cut method of model parameter estimation and the rigorous, dynamic modelling approach to simulate SMB process behaviour are an efficient tool to predict and optimize SMB processes without great experimental efforts. Nevertheless, accuracy is naturally not as high as it could be with more sophisticated methods to determine the model parameters. Further verifications with difficult enantioseparations are necessary to rely on this design approach with as few as possible pilot plant experiments.

6. Notation

α	Separation factor
a_i	First Langmuir coefficient, component i
b_i	Second Langmuir coefficient, component i (m^3/kg)
c_i	Fluid phase concentration, component i (kg/m^3)

c_{Pi}	Concentration in the adsorbent pores, component i (kg/m^3)
D_L	Axial dispersion coefficient (m^2/s)
ϵ	Voidage
$k_{eff,i}$	Effective, overall mass transfer coefficient, component i (m/s)
P_i	Pre Langmuir coefficient, component i
q_i	Load of the particle, component i (kg/m^3)
R_P	Radius of the adsorbent particles (m)
t	Time (s)
v	Interstitial fluid velocity (m/s)
z	Axial space coordinate (m)

References

[1] D.B. Broughton, Chem. Eng. Prog. 64 (1968) 60–65.
[2] K. Unger (Editor), Handbuch der HPLC, Teil 2, GIT Verlag, Darmstadt, 1994.
[3] G. Guiochon, S. Golshan-shirazi, M. Katti, Fundamentals of Preparative and Nonlinear Chromatography, Academic Press, Boston, MA, 1994.
[4] J. Strube, H.-I. Paul, H. Schmidt-Traub, Chem.-Ing.-Tech. 67 (1995) 323–326.
[5] J. Strube, H. Schmidt-Traub, Computers Chem. Eng. 20Suppl. (1996) S641–646.
[6] D.M. Ruthven, C.B. Ching, Chem. Eng. Sci. 44 (1989) 1011–1038.
[7] G. Storti, M. Masi, S. Carrà, M. Morbidelli, Chem. Eng. Sci. 44 (1989) 1329–1345.
[8] G. Storti, M. Mazzotti, M. Morbidelli, S. Carrà, AIChE J. 39 (1993) 471–492.
[9] M. Schulte, J.N. Kinkel, R.-M. Nicoud, F. Charton, Chem.-Ing.-Tech. 68 (1996) 670–683.
[10] J. Strube, U. Altenhöner, M. Meurer and H. Schmidt-Traub, Chem.-Ing.-Tech., 69 (1997) 3.
[11] U. Altenhöner, M. Meurer, J. Strube, H. Schmidt-Traub, J. Chromatogr. A, 769 (1997) in press.
[12] T. Fornstedt, G. Zhong, G. Guiochon, J. Chromatogr. A 742 (1996) 55–68.
[13] M. Schulte, R.M. Devant, A. Keil, F. Charton, Chiral Europe Proceedings, Edinburgh, 1996, in press.
[14] D.M. Ruthven, Principles of Adsorption and Adsorption Processes, Wiley, New York, 1984.
[15] B.-G. Lim, R.B.-H. Tan, C.B. Ching, Sep. Technol. 5 (1995) 213–228.
[16] R.M. Nicoud, LC·GC Int. 5 (1992) 43–47.